Porous inorganic nanocontainers

DOI: 10.1002/anie.200((will be filled in by the editorial staff))

Sub-micron Vaterite Containers: Synthesis, Substance Loading, and Release**

Bogdan V. Parakhonskiy, Albrecht Haase, and Renzo Antolini*

Promising candidates for the development of universal nanoscale delivery systems are porous inorganic nanoparticles[1]. Recently, the applications of porous silicon in a multistage delivery system[2], in polymer coated nanocarriers[3], and of porous silica as core material for lipid bilayers[4] have attracted great attention. A system with similarly high potential, but less studied so far, is porous calcium carbonate in the form of polycrystalline vaterite spheres[5]. It has been shown to exhibit various beneficial properties such as biocompatibility, high drug loading capacity, and preservation of the loaded drugs' properties[6]. However, all these works on $CaCO_3$ were performed with micrometer-sized particles, since the fabrication of nanocontainers turned out to be a big challenge. The common synthesis method of mixing salt solutions allowed producing container sizes of 3 to 15 μm[5b], while the best reproducibility was reached for sizes of about 4 μm[6b, 7] with a porosity of 40%. Yet, the most promising applications demand sub-micrometer size containers, e.g. active coating[8] or drug delivery[9], since smaller sizes favor efficient and homogeneous distribution and give access to micrometer-sized structures like cells or tissue.

Herein we report, for the first time, the fabrication of sub-micron porous vaterite containers, their loading with a probe payload, and its release. Their synthesis is based on crystal growth of polycrystalline, spherical vaterite particles, precipitated from concentrated solutions of $CaCl_2$ and Na_2CO_3[10]. The nucleation and growth rate of the vaterite spheres is determined by the supersaturation level of the dissolved amorphous $CaCO_3$[11]. The final size of the vaterite particles depends strongly on the concentration of the reagents, the solubility of the salts, the reaction time, and the rotation during mixing. It was shown that increasing the concentration of the salts up to 1 M, the rotation speed up to 1500 rpm, and the reaction time to 2 min allowed reducing the vaterite particle size to 3 μm[12]. A particle size reduction beyond these values has so far not been achieved, since vaterite was found to become unstable in water below this critical size, leading to a rapid recrystallization to the calcite phase[13]. This is due to the growing surface-to-volume ratio and enhanced solubility with decreasing particle size.

We resolved this problem by adding ethylene glycol (EG) as a solvent, offering an enhanced density and reduced solubility of $CaCO_3$. This diminished the molecular diffusion, reducing the crystal growth rate and the probability of nucleation, which finally stabilized the vaterite crystals.

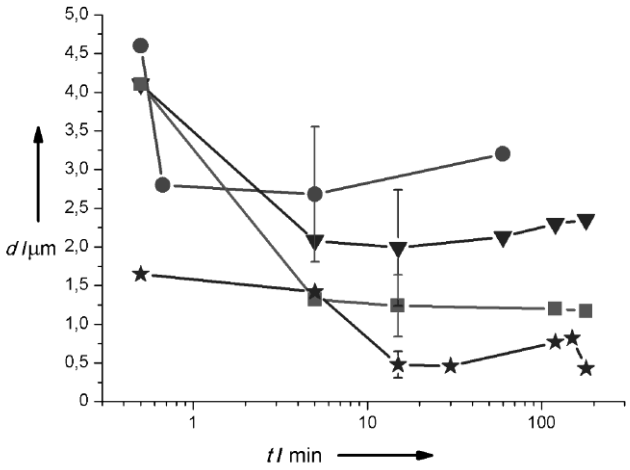

Figure 1. Average diameter of the vaterite particles plotted as a function of the reaction time for various EG concentrations. Graphs correspond to the following immersion solutions: Circle (●) pure water solution; Triangle (▼) 17% ethylene glycol; Square(■) 50% ethylene glycol; Star (★) 83% ethylene glycol. The exemplary error bars show the standard deviations (see Supporting Information).

Experimental evidence of these effects is presented in Figure 1, where the average of the vaterite particle size distribution is shown as a function the reaction time for various EG concentrations. A minimum particle size was obtained at 83% EG concentration and 2 h of mixing, where stable vaterite spheres of 430±10nm average diameter were produced. All size distributions exhibited a constant dispersity[14] of 1.4 (see Supporting Information). The underlying data was obtained by Scanning Electron Microscopy (SEM) (Figure 2a).

As a next step, payload encapsulation into these vaterite sub-micron containers was studied using the fluorescent dye Rhodamine 6G (Rh6G) as a probe substance. Two-photon fluorescence microscopy allowed monitoring the encapsulation and release properties of vaterite particles in various immersion media. This technique offered enhanced signal-to-noise ratio and reduced photobleaching in repeated imaging with respect to confocal microscopy, the much reduced photo-toxicity will be of advantage in future experiments on in-vivo interactions of containers with cells. The optical studies were complemented by zeta potential measurements.

[*] Dr. B. Parakhonskiy, Dr. A. Haase, Prof. R. Antolini
BIOtech – Interdepartmental Center for Biomedical Technologies
University of Trento
Via delle Regole 101,
38123 Mattarello (TN), Italy
E-mail: bogdan.parakhonskiy@gmail.com

[**] We thank F. Piccoli (S. Chiara Hospital, Trento) and F. Tessarolo (BIOtech) for technical assistance with the SEM and T. Bukreeva and L. Feigin (Shubnikov Institute of Crystallography, Russian Academy of Science) for useful discussions. B. P. acknowledges funding by the Provincia autonoma di Trento (Marie Curie Actions, Trentino COFUND).

Supporting information for this article is available on the WWW under http://www.angewandte.org or from the author

Figure 2b shows the Rh6G fluorescence signal from a loaded vaterite container (see also Figure S2). Dye molecules penetrated through the porous structure into the whole crystal. The zeta potential of the bare 430 nm vaterite particles was found to be -26+/-5 mV. In 3 μm vaterite particles this value was found to be -12.2+/-2.5 mV[15], which manifests an increased stability of the sub-micron containers, another favourable feature. After the Rh6G adsorption this value increased to +7 mV.

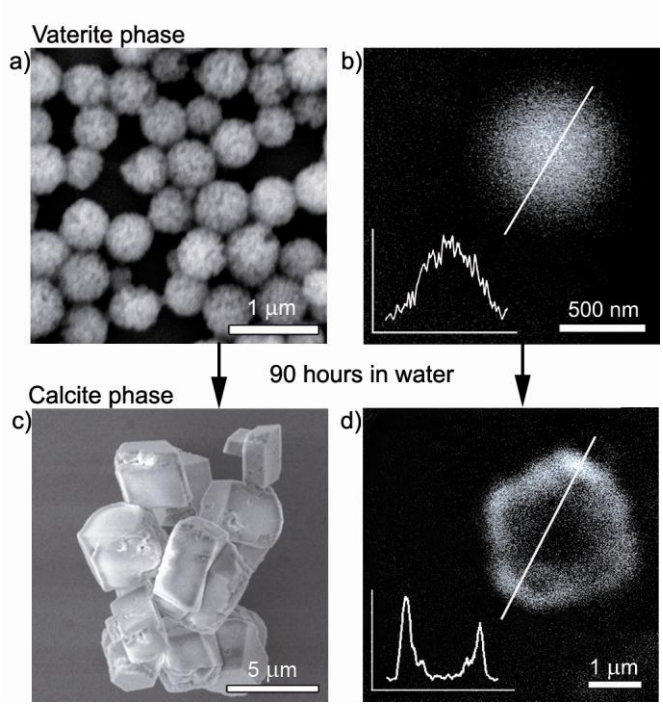

Figure 2. Bimodal microscopic images of the containers: the SEM images show the 430 nm vaterite containers after their synthesis in (a) and the calcite single crystals after recrystallization in (c). The two-photon excited fluorescence images show a single vaterite container loaded with Rh6G in (b) , while in (d) after recrystallization only a residual amount of dye attached to the calcite edges could be observed (see also Figure S1). The insets in (b) and (d) show fluorescence intensity profiles along the marked axes.

Thereafter, payload release was studied using the same techniques. Dye release was observed on two timescales: Firstly, a very slow diminishing of the containers' fluorescence (on the order of weeks) which was found in all immersion media due to desorption of dye molecules from the capsules. Secondly, in aqueous media, a fast drop in fluorescence was observed (within hours), which due to spatial and temporal coincidence can be attributed to a dye release during recrystallization of the vaterite containers (Figure 2a) to calcite (Figure 2c). After recrystallization, residual fluorescence was observed only at the borders of the calcite crystals (Figure 2d), while the dye from the crystal center was dispensed, which is emphasized by the line profile insets in the figures. Large-scale images of loading and release of container clusters are provided in Figure S1. The zeta potential after recrystallization was measured to be 0 mV.

This release process is of special interest, because it can be controlled externally via the immersion medium. Firstly, the time scales of this process have been found to be size-dependent. Generally, they increase with decreasing particle size. Secondly, we investigated in detail the smallest 430 nm containers in diverse immersion media. Figure 3 shows the dynamics of the $CaCO_3$ phase transition. After immersion of the calcite containers in water, recrystallization to calcite sets in after 45 h lasting 44 h. To inhibit recrystallization, containers were immersed in pure ethanol, in this case only the slow dye desorption process was observed, leaving vaterite crystals intact. An acceleration of the recrystallization process was achieved by immersion in sodium chloride. For 0.9 %(w/v) of NaCl, corresponding to physiological saline solution, the time for recrystallization onset decreased to 20 h lasting 41 h. Adding the containers to Phosphate Buffered Saline (PBS, 0.1M, pH 7.4), the recrystallization onset dropped to 4 h lasting 56 h and another crystal structure besides vaterite was found. There are strong indications of this being hydroxyapatite ($Ca_5(PO_4)_3(OH)$)[16]. This new recrystallization mechanism, after an ion exchange reaction with the medium, contributes to the dye release at early times, the time of completion remains the same since the calcite formation time scale seems not affected.

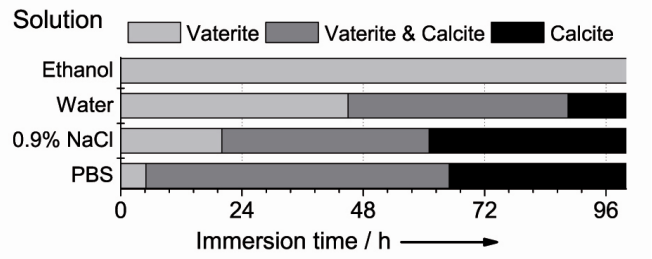

Figure 3. The dynamics of the recrystallization process: In ethanol sub-micron vaterite containers are stable over 100 h, while in water recrystallization to calcite sets in after 45 h and is completed after 89 h. Adding 0,9% NaCl to the solution moves forward the onset and completion of the recrystallization to 20 h and 61 h, respectively. Immersion in PBS (0.1M, pH 7.4) leads to a drop in recrystallization onset to 4 h which is completed after 60 h, in this case besides the transition to calcite, the formation of hydroxyapatite crystals was observed .

In conclusion, it was shown that sub-micron containers can be prepared from vaterite spherical particles, pushing the previous size limit by almost one order of magnitude. Active substances can be loaded under mild conditions into their porous structure, and in an aqueous environment the recrystallization to calcite permits a controlled release. The big advantages of this system are its simplicity and cost-effectiveness, the bio-compatibility, and its universal applicability. For applications requiring further control of the drug release, various coatings can be added to the vaterite containers, as shown in numberless publications (reviewed e.g. by Antipina and Sukhorukov[17]). Depending on the surface modification, the release can then be triggered by change of pH[18, 6b] or temperature[19], by ultrasound[20] or laser illumination[21].

Experimental Section

All utilized chemicals were purchased from Sigma-Aldrich and used without further purification. Spherical colloidal $CaCO_3$ particles were prepared as described by Volodkin[7a]: Amorphous $CaCO_3$ precipitates, formed as a result of colloidal aggregation during rapid mixing of $CaCl_2$ and Na_2CO_3 aqueous solutions, are transformed into ordered spherulites of micrometer sizes. The following processing conditions were chosen: $CaCl_2$ and Na_2CO_3 concentrations of 0.33 M, rotation speed of 500 rpm (with magnetic stirring) at RT, and varying reaction times from 30 s to 3 h;

To prepare sub-micron vaterite spherical particles, Ethylene glycol was added to the reaction solution. To study its influence on the size of the vaterite spheres, the concentration of the EG was varied from 0 to 83% (for the latter, Na_2CO_3 and $CaCl_2$ were dissolved each in 2 ml water and 10 ml EG). When the process was finished,

$CaCO_3$ particles were carefully washed with ethanol and dried for 1 h at 60 °C.

For the encapsulation of Rhodamine 6G, 2 ml of a 1 mg/ml solution of the dye where added to 30 mg dried vaterite containers, the uptake happened during 30 min of shaking. After centrifuging with 3200 x g for 3 min, the remaining free dye molecules where washed off 3 times with ethanol, then the sample was dried again for 3 h at 60 °C. The dry sub-micron containers could be stored for at least 30 days without any sign of degradation. Storage in ethanol gave equally good result.

To study the containers' morphology, a XL 30 field emission environmental scanning electron microscope (FEI-Philips) was used. Size distribution of the vaterite containers and the transition between vaterite and calcite phase were imaged with magnifications from 5000x to 50000x. Statistical image analysis was performed using ImageJ (NIH, http://rsb.info.nih.gov/ij/) based on *N*=100 particles per sample.

The optical studies of the encapsulation and the release processes were performed using a two-photon laser scanning microscope (Ultima IV, Prairie Technologies) with a 100x objective (NA 1.0, water immersion, Olympus) and an ultra-short pulsed laser (Mai Tai Deep See HP, Spectra-Physics) as an excitation source at 840 nm wavelength. The adsorption of the fluorescent probe was controlled by zeta potential measurement using a particle size analyzer (Delsa, Beckman Coulter).

Received: ((will be filled in by the editorial staff))
Published online on ((will be filled in by the editorial staff))

Keywords: nanoparticles · drug delivery · encapsulation · microscopy · controlled release

[1] a) L. J. De Cock, S. De Koker, B. G. De Geest, J. Grooten, C. Vervaet, J. P. Remon, G. B. Sukhorukov, M. N. Antipina, *Angew. Chem.* **2010**, *122*, 7108–7127; *Angew. Chem. Int. Ed.* **2010**, *49*, 6954-6973; b) M. Arruebo, *Wiley Interdiscip. Rev. Nanomed. Nanobiotechnol.* **2011**.

[2] E. Tasciotti, X. Liu, R. Bhavane, K. Plant, A.D. Leonard, B.K. Price, M.M.-C. Cheng, P. Decuzzi, J.M. Tour, F. Robertson, M. Ferrari, *Nat. Nanotechnol.* **2008**, *3*(3), 151-157.

[3] J.-H. Park, L. Gu, G. von Maltzahn, E. Ruoslahti, S.N. Bhatia, M.J. Sailor, *Nat. Mater.* **2009**, *8*(4), 331-336.

[4] C.E. Ashley et al., *Nat. Mater.* **2011,** *10*(5), 1-9.

[5] a) L. Dupont, F. Portemer, M. Figlarz, *J. Mater. Chem.* **1997**, *7*, 797-800; b) Y. Wang, A.D. Price, F. Caruso, *J. Mater. Chem.* **2009**, *19*, 6451-6464.

[6] a) G.B. Sukhorukov, D.V. Volodkin, A.M. Gunther, A.I. Petrov, D.B. Shenoy, H. Möhwald, *J. Mater. Chem.* **2004**, *14*(14), 2073-2081; b) D.V. Volodkin, R. von Klitzing, H. Möhwald, *Angew. Chem.* **2010**, *122*, 9444–9447; *Angew. Chem. Int. Ed.* **2010**, *49*, 9258-61.

[7] a) D.V. Volodkin, A.I. Petrov, M. Prevot, G.B. Sukhorukov, *Langmuir* **2004**, *20*(8), 3398-3406; b) A.A. Antipov, D. Shchukin, Y. Fedutik, A.I. Petrov, G.B. Sukhorukov, H. Möhwald, *Colloids Surf., A* **2003**, *224*, 175-183; c) C. Peng, Q. Zhao, C. Gao, *Colloids Surf., A* **2010**, *353*(2-3), 132-139.

[8] D. G. Shchukin & H. Möhwald, *Small* **2007**, *3*(6), 926-43.

[9] a) J. Panyam, V. Labhasetwar, *Adv. Drug Delivery Rev.* **2003**, *55*, 329–347; b) M. Sokolsky-Papkov, K. Agashi, A. Olaye, K. Shakesheff, A.J. Domb, *Adv. Drug Delivery Rev.* **2007**, *59*, 187-206.

[10] J.P. Andreassen, *J. Cryst. Growth* **2005**, 274(1-2), 256-264.

[11] L. Brecevic, A.E. Nielsen, *J. Cryst. Growth* **1989**, *98*, 504-510.

[12] D. Volodkin, PhD thesis, Lomonosov Moscow State University (Russia), **2005.**

[13] F.-W. Yan, S.-F. Zhang, C.-Y. Guo, X.-H. Zhang, G.-C. Chen, F. Yan, G.-Q. Yuan, *Cryst. Res. Technol.* **2009**, *44*, 725-728.

[14] R. F.T. Stepto, *Pure Appl. Chem.* **2009**, *81*, 351-353.

[15] D.V. Volodkin, N.I. Larionova, G. Sukhorukov, *Biomacromolecules* **2004**, *5*, 1962-72.

[16] A.C. Tas, *Int. J. Appl. Ceram. Technol.* **2007**, *4*, 152-163.

[17] M.N. Antipina, G.B. Sukhorukov, *Adv. Drug Deliv. Rev.* **2011**, *63*, 716-29.

[18] a) G. Sukhorukov, a Fery, H. Möhwald, *Prog. Polym. Sci.* **2005**, *30*, 885-897; b) A. Antipov, G. Sukhorukov, S. Leporatti, I. Radtchenko, E. Donath, H. Möhwald, *Colloids Surf., A* **2002**, *200*, 535- 541.

[19] a) K. Köhler, H. Möhwald, G.B. Sukhorukov, *J. Phys. Chem. B* **2006**, *110*, 24002-10; b) K. Köhler, D.G. Shchukin, H. Möhwald, G.B. Sukhorukov, *J. Phys. Chem. B* **2005**, *109*, 18250-9.

[20] a) H.-J. Kim, H. Matsuda, H. Zhou, I. Honma, *Adv. Mater.* **2006**, *18*, 3083-3088; b) A.M. Yashchenok, M. Delcea, K. Videnova, E. a Jares-Erijman, T.M. Jovin, M. Konrad, H. Möhwald, A.G. Skirtach, *Angew. Chem*. **2010** *122*, 8293–8297; *Ang. Chem. Int. Ed.* **2010** *49*, 8116-8120.

[21] a) A.G. Skirtach, A. Muñoz Javier, O. Kreft, K. Köhler, A. Piera Alberola, H. Möhwald, W.J. Parak, G.B. Sukhorukov, *Ang. Chem*. **2006** 118, 4728–4733; *Ang. Chem. Int. Ed.* **2006** 45, 4612–4617; b) A.G. Skirtach, P. Karageorgiev, M.F. Bédard, G.B. Sukhorukov, H. Möhwald, *J. Am. Chem. Soc.* **2008**, *130*, 11572-11573; c) R. Palankar, A.G. Skirtach, O. Kreft, M. Bédard, M. Garstka, K. Gould, H. Möhwald, G.B. Sukhorukov, M. Winterhalter, S. Springer, *Small* **2009**, *5*, 2168-2176.

Supplementary Information:

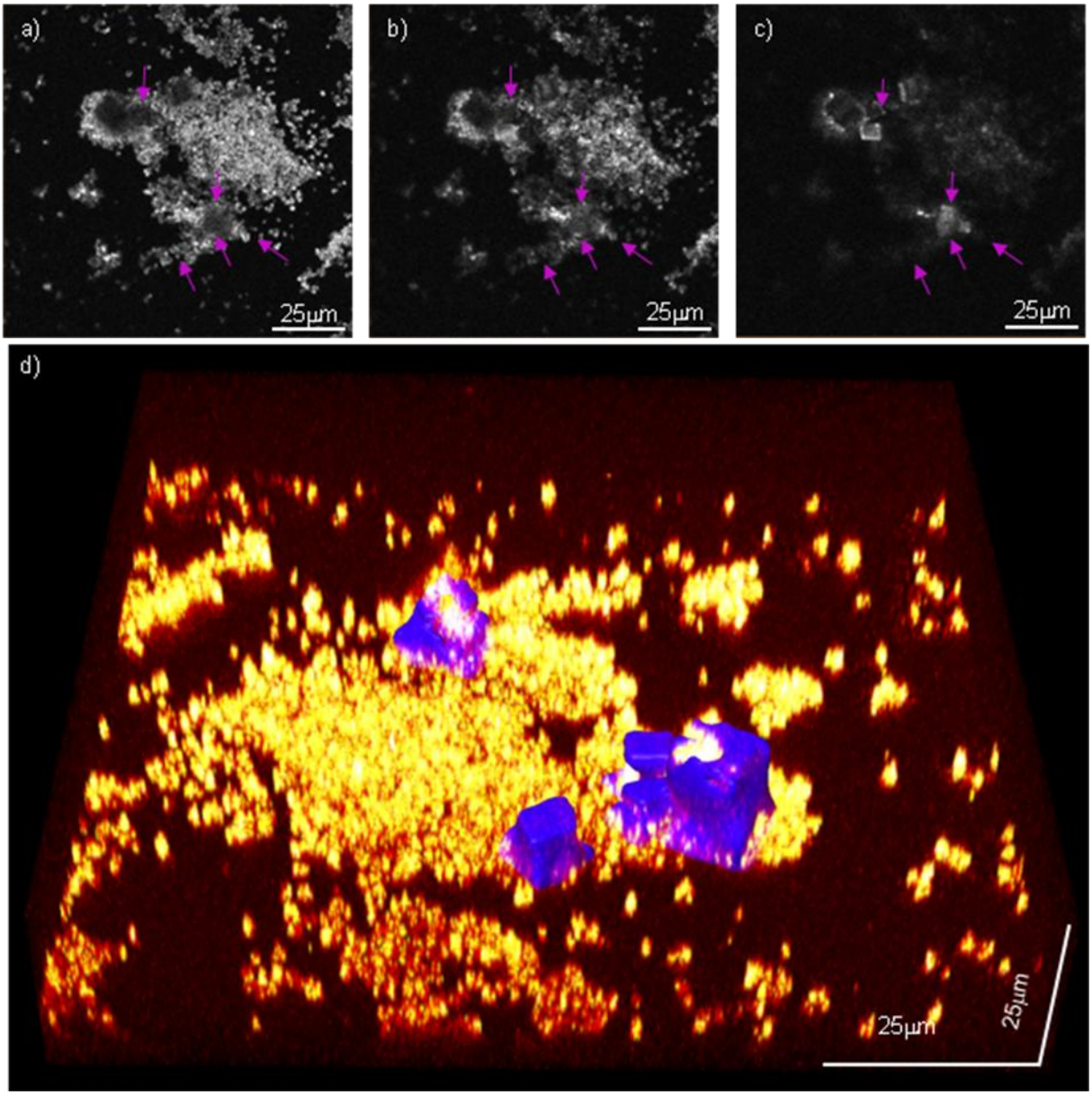

Figure S1 2PM Images of the recystallization/dye release phase. Figures (a-c) show images of a cluster of loaded vaterite capsulas at 2 mm axial distance.The bright fluorescing spheres are dye-loaded containers, while single calcite monocrystals can be localized as dark shadows if the image plane crosses their centers, from which the dye was released, or framed by residual fluorescence when imaged along their surfaces. The calcite positions are marked by arrows. In Figure (d) the whole image stack is shown in a 3D view, the calcite crystals have been highlighted in blue. They show residual fluorescence only at some of the the edges. The appearence of calicite monocrystals and the strong drop in fluorescence are spatially and temporally correlated in all imaged samples, which indicates that the dye release is driven by the recystallization.

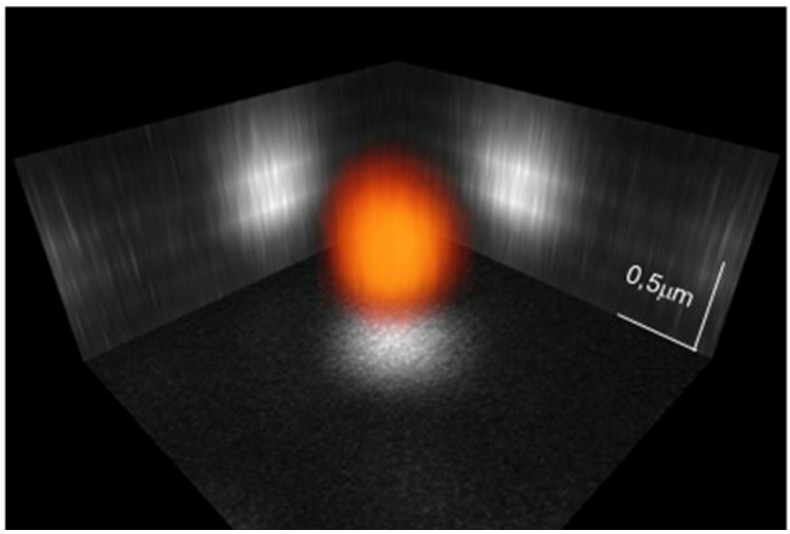

Figure S2, Two-photon volume image and projections of a single vaterite capsula. The image stack contained 6images at 1mm distence which have been linearly interpolated, then a Gaussian filter (*s*=10nm) was applied, an finally the 3D image were deconvoluted with the microscope's Point Spread Function ($s_{x,y}$=0.23mm, s_z=1.12mm). Due to the defraction limit, this image allows only to estimate the total size of the capsulas, the precise size analysis were performed with SEM.

Statistical analysis of the SEM images:

From each probe, $N\cong100$ spheres were chosen randomly, their diameters were measured and averaged. The average diameters are plotted in the paper's Figure 1 with exemplary errorbars representing the **standard deviation** of the sheres' size distributions. For sake of completeness we reproduce in Figure S3 the same graph with all errors.

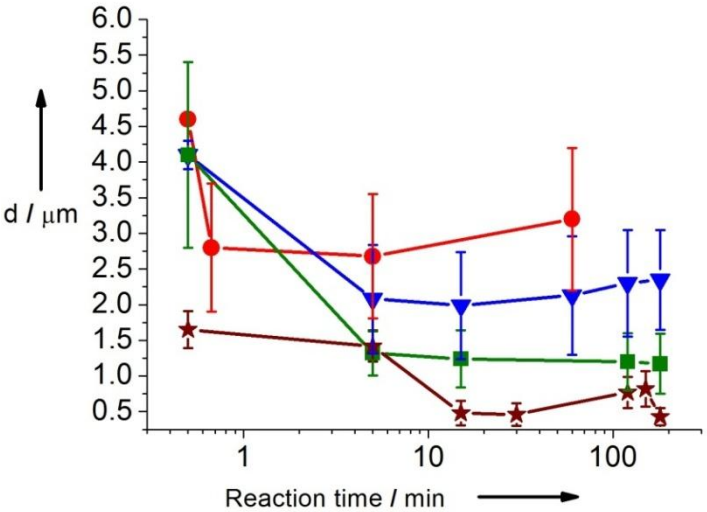

Figure S3, Average diameter of the vaterite particles plotted as a function of the reaction time for various EG concentrations. Graphs correspond to the following immersion solutions: Circle (●) pure water; Triangle (▼) 17% ethylene glycol; Square(■) 50% ethylene glycol; Star (★) 83% ethylene glycol.

Evaluating all the data, we found that the size distributions of the capsulas can be universally described by a single parameter, the **dispersity** (*Đ*) which, assuming constant density, can be defined as the **weight average** of the capsulas volumes divided by the **number average** which we found to be constant for all samples, independent of reaction time or solution medium. *Đ* was calculated from the size distribution as follows:

$$Đ = \frac{\bar{V}_w}{\bar{V}_n} = \frac{\sum_i V_i^2 p_i}{\sum_i V_i p_i}\left(\frac{\sum_i V_i p_i}{\sum_i p_i}\right)^{-1} = \frac{\sum_i V_i^2 p_i \sum_i p_i}{\left(\sum_i V_i p_i\right)^2} = \frac{\sum_i d_i^6 p_i \sum_i p_i}{\left(\sum_i d_i^3 p_i\right)^2}$$

where p_i are the probabilities of the volumes and diameters, V_i and d_i,respectively.

Full reference [4]:

C.E. Ashley, E.C. Carnes, G.K. Phillips, D. Padilla, P.N. Durfee, P. a Brown, T.N. Hanna, J. Liu, B. Phillips, M.B. Carter, N.J. Carroll, X. Jiang, D.R. Dunphy, C.L. Willman, D.N. Petsev, D.G. Evans, A.N. Parikh, B. Chackerian, W. Wharton, D.S. Peabody, C.J. Brinker, *Nat. Mater.* **2011**, *10*, 1-9.